Toward quantitative modeling of silicon phononic thermocrystals

V. Lacatena, M. Haras, J.F. Robillard, S. Monfray, T. Skotnicki, Emmanuel Dubois

Applied Physics Letters

Toward quantitative modeling of silicon phononic thermocrystals

Cite as: Appl. Phys. Lett. **106**, 114104 (2015); https://doi.org/10.1063/1.4915619
Submitted: 19 December 2014 • Accepted: 10 March 2015 • Published Online: 19 March 2015

V. Lacatena, M. Haras, J.-F. Robillard, et al.

AIP Publishing

Toward quantitative modeling of silicon phononic thermocrystals

V. Lacatena,[1,2] M. Haras,[2] J.-F. Robillard,[2,a)] S. Monfray,[1] T. Skotnicki,[1] and E. Dubois[2]
[1]*STMicroelectronics, 850, rue Jean Monnet, F-38926 Crolles, France*
[2]*IEMN UMR CNRS 8520, Institut d'Electronique, de Microélectronique et de Nanotechnologie, Avenue Poincaré, F-59652 Villeneuve d'Ascq, France*

(Received 19 December 2014; accepted 10 March 2015; published online 19 March 2015)

The wealth of technological patterning technologies of deca-nanometer resolution brings opportunities to artificially modulate thermal transport properties. A promising example is given by the recent concepts of "thermocrystals" or "nanophononic crystals" that introduce regular nano-scale inclusions using a pitch scale in between the thermal phonons mean free path and the electron mean free path. In such structures, the lattice thermal conductivity is reduced down to two orders of magnitude with respect to its bulk value. Beyond the promise held by these materials to overcome the well-known "electron crystal-phonon glass" dilemma faced in thermoelectrics, the quantitative prediction of their thermal conductivity poses a challenge. This work paves the way toward understanding and designing silicon nanophononic membranes by means of molecular dynamics simulation. Several systems are studied in order to distinguish the shape contribution from bulk, ultra-thin membranes (8 to 15 nm), 2D phononic crystals, and finally 2D phononic membranes. After having discussed the equilibrium properties of these structures from 300 K to 400 K, the Green-Kubo methodology is used to quantify the thermal conductivity. The results account for several experimental trends and models. It is confirmed that the thin-film geometry as well as the phononic structure act towards a reduction of the thermal conductivity. The further decrease in the phononic engineered membrane clearly demonstrates that both phenomena are cumulative. Finally, limitations of the model and further perspectives are discussed. © *2015 AIP Publishing LLC*.
[http://dx.doi.org/10.1063/1.4915619]

Silicon nanoscale structures are currently being investigated from a rather unconventional point of view: thermoelectric (TE) generation. Indeed, while silicon is known to be the keystone of today's information and communication driving technology, namely, Complementary Metal Oxide Semiconductor (CMOS), its high Seebeck coefficient, 400 μV K^{-1} for 1.7×10^{19} cm^{-3} p-doped silicon,[1] is rarely mentioned. As a matter of fact, silicon features a very high thermal conductivity (148 W m^{-1} K^{-1} @ 300 K) such that a sufficient heat gradient cannot be sustained across devices based on this material which turns to be a very poor TE material. As an example, naturally disordered materials such as $Si_{1-x}Ge_x$ feature a 20 times lower thermal conductivity[2] and are used in high operating temperature TE generators. Since the phonon mean free path distribution peaks in the hundreds of nm range at 300 K, nanoscale patterning, through the introduction of phonon confinement, surface effects, or interferences, is an alternative way to obtain artificially such low thermal conductivity materials. In addition, such a material could preserve the electric conductivity related to the crystalline structure of silicon for the reciprocal reason that the average electron mean free path is estimated to a few nm at room temperature.[1] These approaches use the transition from the ballistic to the diffusive regime as a leverage and are often referred to as *phonon engineering*. Several reports have demonstrated such effects in thin-films,[3] nanowires,[4] and holey membranes.[5,6] Recently, Yu *et al.* published a thorough study of various silicon based nanostructures among which a periodic nano-holes membrane exhibits the lowest conductivity around 2 W m^{-1} K^{-1} with low electric properties degradation.[7] Such a material, combined with an efficient membrane design integrated converter, is expected to push silicon among state-of-the-art TE materials.[8]

Nevertheless, before the accomplishment of this goal, some challenges have to be solved such as the establishment of an efficient and predictive modeling tool for the correct design of the artificial material. As a matter of fact, the origin of the 100-fold reduction in the membrane phononic crystals (PCs) by itself is still debated. While some authors claim that band folding effects (frequency band gaps and group velocity reduction) sometimes named "coherent effects," play a major role[3,9] in thermal conductivity reduction, others pledge that the introduction of inclusions, which scale as the bottom of the thermal conductivity accumulation curve, is the main explanation.[5–7] Indeed, thermal phonons with mean free paths comprised between 40 nm and 40 μm account for 80% of silicon thermal conduction.[9] In the following, the term "phononic" has the broader meaning of a structure which acts on the thermal phonons propagation whether this effect arise from band folding or scattering by the inclusions. In semiconductors, near room temperature, thermal conductivity is dominated by phonon scattering processes. In principle, thermal conductivity can be derived from the Boltzmann transport equation (BTE), but it requires a few assumptions over the phonon dispersion curves and/or the use of *ad hoc* semi-empirical models for the computation of phonon lifetime distribution. Plane wave expansion (PWE) and finite elements methods enable the calculation of the band structures of phononic crystals. However, the linear elasticity hypothesis cannot account for phonon-phonon interactions that

a)jean-francois.robillard@isen.iemn.univ-lille1.fr

result from anharmonicity and give its finite value to the thermal conductivity.[9] Lattice dynamics offers an alternative method. It requires to calculate the dynamical force constant matrix that describes the interactions between atoms and the successive neighbors in the unit cell in order to calculate the dispersion curves. Then, phonon lifetimes can be computed in the frame of the perturbation theory and used as input for the BTE. Such an analysis can be found for the case of Lennard-Jones argon.[10] This methodology is hardly suitable for large and complex simulation cells since the dynamical matrix has to be determined first by another method.

In this work, we chose Molecular Dynamics (MD) combined with the Green-Kubo method to predict lattice thermal conductivity. Molecular dynamics relies on the use of an interatomic potential to solve the classical motion equations and gather statistical thermodynamic data. This method encompasses all the effects of the anharmonic part of the potential. Especially, all the changes induced in the phonon lifetimes and group velocities can be described with no further assumptions. MD simulations are performed using the LAMMPS software.[11,12] The environment-dependent interatomic potential (EDIP)[13,14] was chosen for its better ability to reproduce thermal conductivity of bulk silicon with respect to other models such as the Stillinger-Weber or Tersoff potentials. A full demonstration of EDIP suitability for studying silicon bulk thermal conductivity is provided in Ref. 15. The frequencies extracted from MD simulations and lattice dynamics calculations are compared with experimental values, showing the satisfactory agreement of the obtained phonon dispersion curves. The simulation cells geometries are aimed at describing bulk, membrane, PC, and phononic membrane (PM) and are schematized in Fig. 1. The bulk cell is an $8 \times 8 \times 8$ silicon lattice constants cube with periodic boundaries in all directions. The membrane cells are $8 \times 8 \times N$ parallelepipeds with $N = 15$, 20, and 30,

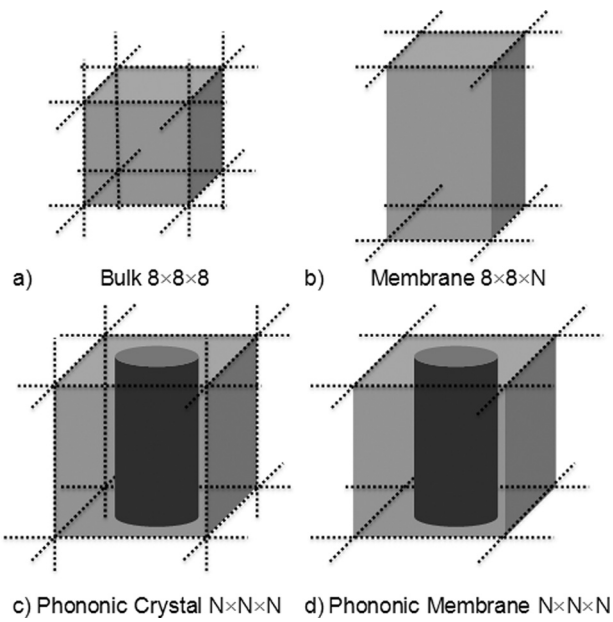

FIG. 1. MD simulation cells used in this work to describe: (a) Bulk silicon, (b) membranes, (c) phononic crystals with infinite z-axis dimensions, and (d) phononic membranes. The figures $X \times Y \times Z$ denotes the cells dimensions in terms of silicon lattice constants.

boundaries are periodic in the x and y directions only. The PC cells are $N \times N \times N$ boxes with periodic boundary conditions in all directions; a cylinder of radius R lattice constants depending on the size N is extruded. This cell describes a 2D N-periodic array of cylinders etched in bulk. Finally, the PM cell combines the $N \times N \times N$ geometry and the periodic boundaries in the x and y directions. The geometrical filling fraction (*ff*), which is a conventional comparison figure for phononic structure, is equal to $\pi R^2/N^2$. All the parameters (N, R, *ff*) are reported in Table I.

The choice of simulating perfectly periodic structures matches both experimental fabrication constraints and efficient computation time in simulations. The dimensions were chosen as a tradeoff between reasonable computation time and meaningful dimensions. Indeed, the 15 lattice constants correspond to a thickness of 8.5 nm which is the experimental state-of-the-art for ultrathin silicon membranes.[16] However, the lateral dimensions are still low as compared to actual phononic materials for which pitch scales as 40 nm at best.[7,17]

The simulation time step is 0.5 fs. A first simulation stage, using NPT ensemble with a Nosé-Hoover thermostat at $T = 300$, 350, and 400 K and barostat at zero pressure, aims at finding the equilibrium configurations. Indeed, the interfaces introduce local stress, which need to be unclenched before further analysis. During this stage, the cell dimensions in all directions are averaged until equilibrium is reached (from 5 to 10 ns) in order to determine the lattice constant. In the bulk case, the three dimensions are coupled to simulate a hydrostatic pressure tensor. In all other cases, since the cells have different boundary conditions along the z axis, the x and y dimensions are coupled while the z dimension is independent. Having obtained an equilibrium configuration, the velocities are then randomized following a Gaussian distribution, in order to simulate ten independent systems for each set of parameters and compute satisfactory statistics. An additional NVT 10 ps run is then applied before the NVE ensemble is established and the heat current autocorrelation function is accumulated following the Green-Kubo formalism until sufficient convergence (10 ns). More details about this methodology can be found in Ref. 18.

Figure 2 shows a set of simulation summarizing the results. First, the bulk value of the silicon thermal conductivity is well reproduced.[19] At temperatures higher than 300 K,

TABLE I. Cells dimensions, filling fraction, and simulated thermal conductivities at 300 K.

Type/boundaries	Size N	Radius R	*ff* (%)	κ (W/m/K) *p p p*	κ (W/m/K) *p p s*
Bulk $8 \times 8 \times 8$	…	…	…	165.7	…
Membrane$8 \times 8 \times N$	15	…	…	…	44.9
	20	…	…	…	54.2
	30	…	…	…	59.3
PC and PMN $\times$ N $\times$ N	15	3	12.57	19,82	12,03
	15	4	22.34	9.51	7.22
	15	5	34.91	5.76	4.11
	15	6	50.27	2.24	2.36

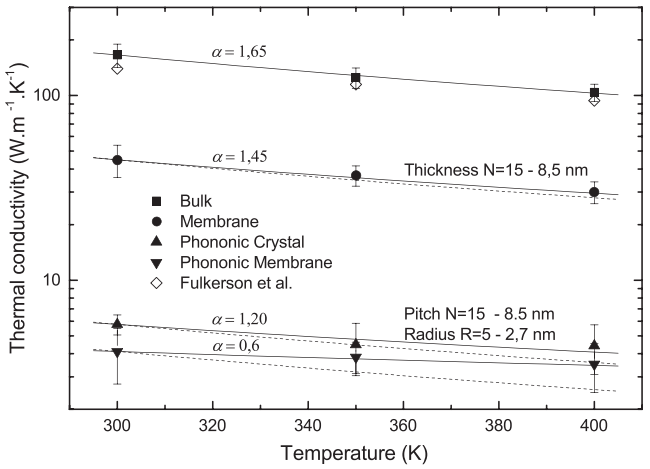

FIG. 2. Simulated thermal conductivity as a function of temperature (plain symbols). The results are fitted according to the model described by Eq. (1) (solid lines). A comparison to several experimental results from literature[19] is shown (white symbols).

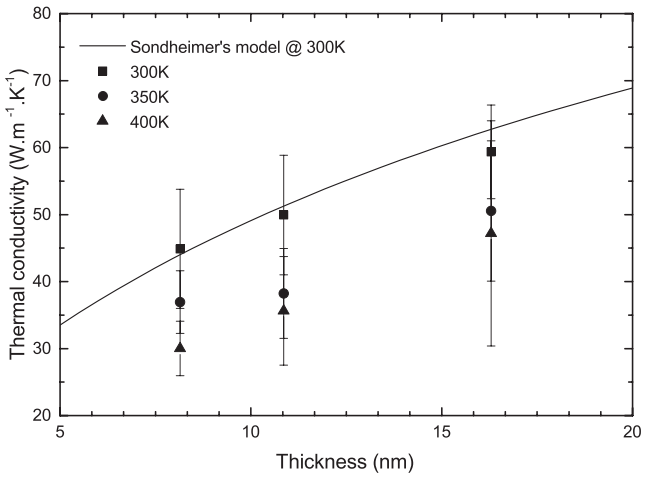

FIG. 3. Thermal conductivity as a function of membranes thickness for three different temperatures. The results for 300 K are fitted using the Fuchs-Sondheimer model[24,25] for a mean free path of 300 nm and a value of the specularity parameter $p = 0.75$. The value of p chosen is in agreement with calculation and experimental measurements by Maldovan.[3]

the thermal conductivity of semiconductors is known to decay following a power law:[20]

$$\kappa = \kappa_{300K}\left(\frac{T_0}{T}\right)^{\alpha}, \tag{1}$$

where κ_{300K} is the thermal conductivity at $T_0 = 300$ K. Equation (1) has been plotted using the coefficient $\alpha = 1.65$ from Palankovski's work.[21] The agreement between simulation and this model is remarkable for bulk. For the membranes and phononic crystals, the accordance remains within the error bars. Though, an effect is clearly seen that flattens the thermal conductivity curve as a function of temperature. Such a behavior is well known to occur in low dimension silicon structures[22] and it is noticeable that it is accounted for by the simulation procedure. Indeed, tuning down the α coefficient as indicated in Figure 2 enables a precise fitting of the results. This procedure could provide insight about the way anharmonic processes are affected by dimensionality since the exact value of α is mainly governed by the third and fourth order anharmonic parts of the potential.[23]

On another hand, Figure 2 shows a decrease of the thermal conductivity from bulk to thin film geometry (44.9 W m^{-1} K^{-1}) and phononic crystal geometries (5.76 W m^{-1} K^{-1}). It is noticeable that, despite the phononic crystal being infinite along the z axis, this configuration achieves a 30 times reduction of κ with respect to bulk. The same order of magnitude is obtained for all phononic crystals whatever the pitch. This result supports several experimental observations of reduced thermal conductivity in relatively thick silicon membranes[6] and is of great relevance for practical use in the frame of micro-integrated thermoelectric devices.[8,17] Finally, a further reduction is observed for phononic membranes (4.11 W m^{-1} K^{-1}), which demonstrates that both effects cumulate in such systems. This last result is all the more relevant that it takes into account and evaluate the respective contributions of the thin film geometry and the phononic structure with no need for further hypothesis or *ad hoc* parameter.

Detailed results for plain membranes are shown in Fig. 3. As expected, the thermal conductivity of thinner membranes is reduced. This is usually explained in terms of phonon confinement and surface scattering that limits the thermal phonons mean free path. The same trend is noticed for all temperatures and reproduced using the Fuchs-Sondheimer model[24,25] (Eq. (1), solid line in Fig. 3)

$$\frac{\kappa_{memb.}}{\kappa_{bulk}} = \left(1 - \frac{3(1-p)}{2\delta}\right) \cdot \int_1^{\infty} \left(\frac{1}{\xi^3} - \frac{1}{\xi^5}\right) \cdot \frac{1 - e^{-\frac{t}{\Lambda}\xi}}{1 - pe^{-\frac{t}{\Lambda}\xi}} \cdot d\xi, \tag{2}$$

where t is the thickness, $\Lambda = 300$ nm is the mean free path at 300 K (Ref. 21), and $p = 0.75$ is the fraction of phonons specularly reflected at the boundaries.

Figure 4 stresses the influence of the holes on thermal conductivity. It is worth noticing how increasing the filling

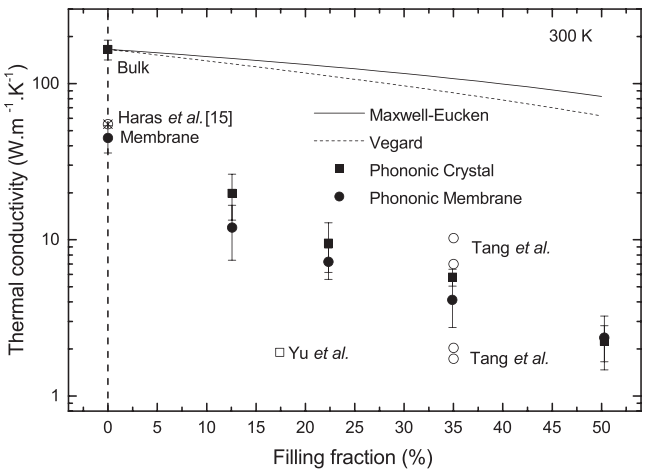

FIG. 4. Thermal conductivity as a function of filling fraction *ff* for periodic patterns in bulk (squares) and thin film membranes (circles) at 300 K. Maxwell-Eucken and Vegard models of porous media are indicated and clearly show that phononic engineering is far more efficient than the sole material removal effect. A comparison to several experimental results from literature[5,7,27] is shown (white symbols).

fraction (by increasing the radius of the enclosures) induces a further reduction of the thermal conductivity. Because the Green-Kubo methodology provides quantitative information from a statistical analysis, it is difficult to discriminate the microscopic processes leading to the conductivity reduction. The commonly cited effects are band gap opening, group velocity reduction due to band folding, and increased diffusion on boundaries. Band gaps usually arise in the lower frequency range of the band folded dispersion curves. Thus, even a pitch as low as 8.5 nm would not produce a gap above 1 THz. Furthermore, square lattices symmetry is not usually suitable to obtain large band gaps,[26] unless very high filling fractions are achieved. It is unlikely that the structures studied here exhibit any phononic band gap. Finally, the consequence of local disorder in the periodic structure is the introduction of propagating modes in the band gap and would reduce its efficiency. Another common interpretation is given in terms of reduced limiting dimensions of the structure.[9] Indeed, as the radius increases, the space between two enclosures forms a bottleneck. The reduced neck size (distance between two consecutive holes) entails an increase of scattering and the consequent decrease of the phonon mean free path. Finally, the mostly cited effect provoking a 2-order of magnitude decrease of κ is the band flattening due to the Brillouin zone folding, related to the artificial crystal periodicity.[9] The methodology described in this letter correctly encompasses the effects of the thin film geometry, cylindrical enclosures, and possible periodic effects. However, the two later contributions remain intricate. Indeed, discriminating the effect of periodicity with respect to scattering on the cylindrical patterns would require to relax periodic boundary conditions and to simulate a randomized holes distribution at high computational cost.

From the quantitative point of view, the order of magnitude matches experiments such au Yu *et al.*[7] ($1.9\,W\,m^{-1}\,K^{-1}$) and Tang *et al.*[5] (from 1.73 to $10.23\,W\,m^{-1}\,K^{-1}$). Though, several discrepancies exist between these experiments and the systems studied in this paper. The most critical being the limited dimensions of the simulation cell related to computational limitations. Interestingly, all the remaining effects that could be taken into account should further hinder the phonon transport and reduce thermal conductivity. Green-Kubo methodology provides a classical description of specific heat for temperatures below the Debye's one. Thus, it slightly overestimates the thermal conductivity, which could be compensated by quantum corrections. Defects, impurities, and isotopic composition are known to be other factors toward low conductivity. Last but not least, the native silicon dioxide layer formed at the silicon surfaces exposed to air could likely account for the difference between the plain silicon conductivity modeled with MD and the value obtained by experiments. All these effects can be appropriately treated in the frame of MD simulations or estimated. Thus, better matching of simulated values with respect to experiments mainly relies on the capacity to achieve realistic cell dimensions that in turn require sufficient computation capability.

In summary, the impressive reduction of silicon thermal conductivity due to nanoscale periodic patterning is well reproduced by means of a Green-Kubo MD methodology using the EDIP potential. Furthermore, the results highlight the suitability of MD toward quantitative comparison to experimental values. Neither assumptions on the phonon distribution nor on the transport mechanisms are necessary. The method is demonstrated to reproduce several experimental trends, such as the temperature and the dimensionality effects, which shed light onto the thermal transport in nanoscale systems. The findings clearly show that the phononic structure accounts for a significant part of the thermal conductivity reduction with respect to the thin film geometry. This fact is in agreement with several experimental reports and is of crucial importance for application in thermoelectric device design.

The research leading to these results has received funding from the European Research Council under the European Community's Seventh Framework Programme (FP7/2007-2013) ERC Grant Agreement No. 338179. V. Lacatena and M. Haras received financial support from the ANRT for CIFRE research grants in the frame of the STMicroelectronics-IEMN common laboratory. The authors gratefully acknowledge E. Lampin for fruitful discussions. The authors acknowledge GENCI for access to high performance computer CURIE.

[1]L. Weber and E. Gmelin, Appl. Phys. A: Mater. Sci. Process. **53**, 136 (1991).
[2]B. Abeles, Phys. Rev. **131**, 1906 (1963).
[3]M. Maldovan, J. Appl. Phys. **110**, 034308 (2011).
[4]A. I. Boukai, Y. Bunimovich, J. Tahir-Kheli, J.-K. Yu, W. A. Goddard III, and J. R. Heath, Nature **451**, 168 (2008).
[5]J. Tang, H.-T. Wang, D. H. Lee, M. Fardy, Z. Huo, T. P. Russell, and P. Yang, Nano Lett. **10**, 4279 (2010).
[6]P. E. Hopkins, C. M. Reinke, M. F. Su, R. H. Olsson, E. A. Shaner, Z. C. Leseman, J. R. Serrano, L. M. Phinney, and I. El-Kady, Nano Lett. **11**, 107 (2011).
[7]J.-K. Yu, S. Mitrovic, D. Tham, J. Varghese, and J. R. Heath, Nat. Nanotechnol. **5**, 718 (2010).
[8]M. Haras, V. Lacatena, S. Monfray, J.-F. Robillard, T. Skotnicki, and E. Dubois, J. Electron. Mater. **43**, 2109 (2014).
[9]E. Dechaumphai and R. Chen, J. Appl. Phys. **111**, 073508 (2012).
[10]J. E. Turney, E. S. Landry, A. J. H. McGaughey, and C. H. Amon, Phys. Rev. B **79**, 064301 (2009).
[11]S. Plimpton, J. Comput. Phys. **117**, 1 (1995).
[12]See http://lammps.sandia.gov for a detailed description and source codes.
[13]J. F. Justo, M. Z. Bazant, E. Kaxiras, V. V. Bulatov, and S. Yip, Phys. Rev. B **58**, 2539 (1998).
[14]M. Z. Bazant, Ph.D. thesis, Harvard University, Cambridge, 1997.
[15]A. S. Henry and G. Chen, J. Comput. Theor. Nanosci. **5**, 141–152 (2008).
[16]J. Cuffe, E. Chaávez, A. Shchepetov, P.-O. Chapuis, E. H. El Boudouti, F. Alzina, T. Kehoe, J. Gomis-Bresco, D. Dudek, Y. Pennec, B. Djafari-Rouhani, M. Prunnila, J. Ahopelto, and C. M. Sotomayor Torres, Nano Lett. **12**, 3569 (2012).
[17]V. Lacatena, M. Haras, J.-F. Robillard, S. Monfray, T. Skotnicki, and E. Dubois, Microelectron. Eng. **121**, 131 (2014).
[18]P. C. Howell, J. Chem. Phys. **137**, 224111 (2012).
[19]W. Fulkerson, J. P. Moore, R. K. Williams, R. S. Graves, and D. L. McElroy, Phys. Rev. **167**, 765 (1968).
[20]N. W. Ashcroft and N. D. Mermin, *Solid State Physics* (Holt, Rinehart and Winston, New York, 1976).
[21]V. Palankovski, R. Schultheis, and S. Selberherr, IEEE Trans. **48**, 1264–1269 (2001).
[22]A. M. Marconnet, M. Asheghi, and K. E. Goodson, J. Heat Transfer **135**, 061601 (2013).
[23]C. Herring, Phys. Rev. **96**, 1163 (1954).
[24]K. Fuchs, Proc. Cambridge Philos. Soc. **34**, 100 (1938).
[25]E. H. Sondheimer, Adv. Phys. **1**, 1 (1952).
[26]J. O. Vasseur, P. A. Deymier, B. Djafari-Rouhani, Y. Pennec, and A.-C. Hladky-Hennion, Phys. Rev. B **77**, 085415 (2008).
[27]M. Haras, V. Lacatena, F. Morini, J.-F. Robillard, S. Monfray, T. Skotnicki, and E. Dubois, IEEE Int. Electron Devices Meet. **2014**, 8.5.212.